# Internal dissipation of a polymer

J. M. Deutsch
*Department of Physics, University of California, Santa Cruz, California 95064, USA*
(Received 10 March 2010; published 29 June 2010)

The dynamics of flexible polymer molecules are often assumed to be governed by hydrodynamics of the solvent. However there is considerable evidence that internal dissipation of a polymer contributes as well. Here we investigate the dynamics of a single chain in the absence of solvent to characterize the nature of this internal friction. We model the chains as freely hinged but with localized bond angles and threefold symmetric dihedral angles. We show that the damping is close but not identical to Kelvin damping, which depends on the first temporal and second spatial derivative of monomer position. With no internal potential between monomers, the magnitude of the damping is small for long wavelengths and weakly damped oscillatory time dependent behavior is seen for a large range of spatial modes. When the size of the internal potential is increased, such oscillations persist, but the damping becomes larger. However underdamped motion is present even with quite strong dihedral barriers for long enough wavelengths.

DOI: 10.1103/PhysRevE.81.061804 PACS number(s): 36.20.−r, 81.05.Lg, 82.37.Rs, 82.80.Ms

## I. INTRODUCTION

Polymer molecules in solution are usually modeled assuming that damping is mediated by interaction with surrounding fluid, or other polymer chains. However it has been noted early on, that there is another source of dissipation, internally generated by the nonlinear dynamics of the polymer chain [1–3]. In a set of important experiments [3] extensional relaxation for different solvent viscosities was measured. By extrapolating the solvent viscosities to zero, an interesting residual dissipation was discovered that is internal in origin. A number of explanations for it have been proposed [4,5], but the origins of this effect are still not well understood.

In this work, the internal friction of a polymer is examined by considering it in isolation, that is, without any solvent. This not only sheds light on the case of polymer solutions, but also on more recent experimental techniques, discussed below, used to characterize polymers by first gasifying them without damaging their integrity.

Developments in mass spectrometry of long chain polymers, have become important in recent years in order to characterize large biological molecules such as proteins [6]. The process involved in these experiments puts single chains into a vacuum. The study of polymer damping in this environment would elucidate the understanding of internal dissipation but has yet to be studied experimentally. However recent work has studied the behavior of single chain molecules in a vacuum theoretically and by means of computer simulation [7,8]. The statistical properties of single chains with no damping, and subject only Newton's laws was investigated. Both ideal chains (where only chain connectivity is included and no intrachain interactions), and self-avoiding chains, were considered. In related work, the detailed chaotic properties of small chains with rigid links has also been observed for self-interacting chains with two body Lennard-Jones potentials [9]. Through a comprehensive analysis of this problem, they were able to show that the simulated chains were in excellent agreement with exact predictions from a microcanonical average, providing strong evidence that the dynamics are indeed ergodic. The chaotic motion derives from both the bond constraints and the convex nature of scattering. In another related work [10] computer simulations for polymer molecules were performed to examine Lyapunov exponents. These were shown to be very small for systems close to a phase transition, such as the coil-globule transition.

An ideal chain modeled with only linear springs connecting adjacent monomers is integrable and shows no damping. Energy in every mode is conserved and cannot be exchanged with other modes. Dissipation results from the nonlinear coupling of modes to each other. This is closely related to the problem of nonlinear one dimensional chains that have been studied extensively using the Fermi, Pasta, and Ulam (FPU) model [11]. In this model, there is energy transfer between modes, however depending on initial conditions, the time it takes to lose correlation with its initial state can be very long [12]. An ideal chain is a similar one dimensional system where the displacement of each particle is, in this case, much larger and is vectorial in nature. However we expect that the same equilibration problems persist. Therefore to thermalize a polymer in a vacuum efficiently, the model chosen [7] uses rigid links so that the local motion would be highly chaotic. It also mimics the fact that the fluctuations in bond lengths are small compared to those involved with rotational degrees of freedom. On large length scales however, one might expect universal behavior, independent of the form of the potential connecting adjacent monomers. As will be seen below, this appears to be the case.

The dynamics of such ideal chains are also closely related to the study of the dynamics and energy flow in one dimensional chains, that govern its anomalous conductivity [13,14]. The dynamics in one dimension systems with momentum conservation show faster relaxation than in higher dimensions due to Galilean invariance. A consequence of momentum conservation in higher dimensions is responsible for long time tails in liquids that were predicted theoretically [15] and confirmed experimentally [16]. In the case of one dimensional nonlinear chains, a wide range of different models give the same heat conductivity exponent, for example the Sinai Pencase model [17], the Random Collision Model

 

[14] and FPU chains [18]. The main difference between these one dimensional systems and ideal chains in a vacuum is that the former has a fractal dimension of 1, and the latter, of 2. It is therefore hard to define local hydrodynamic variables as a function of position for polymer chains. However conservation of energy and momentum are common to both problems.

In addition, in the case of an ideal chain in a vacuum, the equilibrium properties are effected by the conservation of angular momentum [8], and this can be analyzed exactly, showing that when the angular momentum is zero, the radius of gyration is significantly smaller than without that conservation law enforced.

Initial results [7] for an ideal chain in a vacuum showed that its dynamics are very different than those of a chain in solution. A freely hinged chain of $N$ links, with constant link lengths was studied. The time autocorrelation function for position oscillates and is slowly damped. The damping time appears to scale as $T_{rel} \propto N^{(1.85 \pm .15)}$, where $L$ is the chain length.

The reason for this behavior can be seen by understanding the form of dissipation such chains should have. Because of Galilean invariance, the frictional force $f_d$ on a monomer cannot be proportional to its velocity, as this would imply that a uniformly translating chain would slow down. If we denote the position of a chain at arclength $s$ as $\mathbf{r}(s)$, then the simplest term respecting this translational invariance is

$$f_d \propto \frac{\partial^3 \mathbf{r}}{\partial t \partial^2 s} \tag{1}$$

This is the form of "Kelvin Damping" [19]. This theoretical form was proposed by MacInnes based on a calculation done by him for a model system [4]. It was later proposed as the origin of Cerf friction [2] where it was argued that this form was compatible with experiments characterizing internal friction [3]. In Fourier space with wave-vector $k$ conjugate to $s$, and $\omega$ conjugate to $t$, this dissipation is proportional to $i\omega k^2 \hat{r}(k,w)$. Longer wavelength modes are weakly damped, implying underdamped motion for long enough wavelengths as we will shortly see. Using this damping along with linear forces between monomers, analogous to the Rouse model [20], one has

$$\rho \frac{\partial^2 \mathbf{r}}{\partial t^2} = \left( \kappa + C \frac{\partial}{\partial t} \right) \frac{\partial^2 \mathbf{r}}{\partial s^2} + \xi(\mathbf{s}, \mathbf{t}). \tag{2}$$

Here $\xi$ is a noise term added to maintain ideal chain statistics. $\rho$ is the mass per unit arclength. The term $\kappa r''(s)$ is identical to that of the Rouse equation and describes the net force experienced from neighboring segments. For Gaussian chains, $\kappa = 3k_B T$, where $T$ is the temperature [1]. For a linear chain, $r'(s)=0$ at the two ends and the chain can be expanded in terms of Fourier modes, similar to the analysis of the Rouse equation

$$\mathbf{r}(s) = \sum_k \hat{\mathbf{r}}_k \cos(ks) \tag{3}$$

with $k = n\pi/L$, $n = 1, 2, \ldots$. so that

$$\rho \frac{\partial^2 \hat{\mathbf{r}}}{\partial t^2} = -k^2 \left( \kappa - C \frac{\partial}{\partial t} \right) \hat{\mathbf{r}} + \hat{\xi}(k,t). \tag{4}$$

When noise is omitted, this is of the form a damped harmonic oscillator with an effective mass of $\rho$, a spring constant of $K = \kappa k^2$ and friction of $\nu = Ck^2$, so that

$$M\ddot{r} + \nu \dot{r} + Kr = 0. \tag{5}$$

For underdamped long wavelength modes, the solution is proportional to $\exp(i\Omega t)$ with $\Omega_k \equiv \omega_k + i\lambda_k$. The correlation function for a $k$ mode can then be calculated

$$\langle r_k(0) r_k^*(t) \rangle = \langle |r_k|^2 \rangle \mathrm{Re}[\exp(i\Omega_k t)\Omega_k/\omega_k]. \tag{6}$$

$\lambda_k \propto k^2$ (in the underdamped regime) so the damping time $\propto 1/k^2$. The frequency of oscillation, $\omega_k$, is proportional to $k$ for small $k$. Therefore in this limit, there are many oscillations, $O(k^{-1})$ in a damping time.

The model of a freely hinged chain is not realistic at a microscopic level. A molecule such as polyethylene has a strong orientational dependence as dihedral angles are varied. The chain will spend most of its time in minima and make transitions between these. The arguments above are general and do not give any indication of the prefactor for the dissipation term. This is expected to depend on the details of the potential. We will use numerical methods to see to what extent Eq. (4) is satisfied and to determine how the size of the prefactor $C$ depends on the potential used. We will find, surprisingly, that underdamped motion is still present even with rather strong potentials. We first describe the numerical method used in this work and then give the simulation results in the following section.

## II. NUMERICAL METHOD

This method is an extension of the simulation of rigid link systems developed by the author previously [21,22] which considered the case of a highly overdamped systems where inertia was negligible. Here we consider the general case of particles with mass $m$ and damping $\gamma$. In the subsequent sections, we will take $\gamma = 0$.

The coordinates are denoted $\mathbf{r}_1, \mathbf{r}_2, \ldots, \mathbf{r}_N$, where $N$ is the number of masses in the system. The time derivative of these, that is the velocities, are denoted $\mathbf{v}_1, \mathbf{v}_2, \ldots, \mathbf{v}_N$. As in the earlier work, we will assume that each mass is being acted on by a force $\mathbf{f}_i$, which can be due to self-interaction or externally applied. It will be convenient to define the difference operator of adjacent coordinates or velocities $\Delta_i \mathbf{r} \equiv \mathbf{r}_{i+1} - \mathbf{r}_i$ and $\Delta_i \mathbf{v} \equiv \mathbf{v}_{i+1} - \mathbf{v}_i$. To keep the link lengths constant, we Introducing Lagrange multipliers $t_1, \ldots, t_{N-1}$ which describe the tensions between neighboring masses, we can write the equations of motion as

$$m\dot{\mathbf{v}}_i + \gamma \mathbf{v}_i = t_i(\Delta_i \mathbf{r}) - t_{i-1}(\Delta_{i-1}\mathbf{r}) + \mathbf{f}_i, \tag{7}$$

$$\dot{\mathbf{r}}_i = \mathbf{v}_i \tag{8}$$

for $1 < i < N$. For a linear chain, one can define $t_0 = t_N = 0$ to give the equations for the chain ends, that is for $i = 1$ and $i = N$. We will discuss ring chains below.

We wish to evolve the $\mathbf{r}$'s and $\mathbf{v}$'s in time by finding the tension at every time step which allows us to iterate the above equations by some appropriate integration scheme. However this can be problematic due to the cumulation of errors, as we require that the magnitude of $\Delta_i\mathbf{r}$ remain very close to the step length, $l$. Define the error in this quantity as

$$\epsilon_i \equiv |\Delta_i\mathbf{r}|^2 - l^2. \tag{9}$$

Without the problem of numerical error, the tensions would be determined by the condition $\epsilon_i=0$ for $i=1,\ldots,N$. By differentiating this equation twice with respect to time, a formula for the tensions can be obtained. However numerical error will cause bond lengths to stray from their initial values. Therefore we need to introduce feedback into the method so that nonzero $\epsilon_i$ will be pushed back toward zero. So instead we consider the equation

$$A\epsilon_i + B\dot{\epsilon}_i + \ddot{\epsilon}_i = 0, \tag{10}$$

where $A$ and $B$ are constants causing a damping of errors with time, and whose values are determined to maximize computational efficiency. This can be rewritten as

$$2\Delta_i\mathbf{r}\cdot\Delta_i\dot{\mathbf{v}} = -A\epsilon_i - 2B\Delta_i\mathbf{r}\cdot\Delta_i\mathbf{v} - 2|\Delta_i\mathbf{v}|^2. \tag{11}$$

Applying the difference operator $\Delta_i$ to Eq. (7) and taking the dot product with $\Delta_i\mathbf{r}$ gives

$$m\Delta_i\mathbf{r}\cdot\Delta_i\dot{\mathbf{v}} + \gamma\Delta_i\mathbf{r}\cdot\Delta_i\mathbf{v} = t_{i+1}\Delta_i\mathbf{r}\cdot\Delta_{i+1}\mathbf{r} + t_{i-1}\Delta_i\mathbf{r}\cdot\Delta_{i-1}\mathbf{r} - 2t_i|\Delta_i\mathbf{r}|^2 + \Delta_i\mathbf{r}\cdot\Delta_i\mathbf{f}. \tag{12}$$

Putting this into Eq. (11) gives

$$t_{i+1}\Delta_i\mathbf{r}\cdot\Delta_{i+1}\mathbf{r} - 2t_i|\Delta_i\mathbf{r}|^2 + t_{i-1}\Delta_i\mathbf{r}\cdot\Delta_{i-1}\mathbf{r} = \frac{m}{2}(-A\epsilon_i - 2B\Delta_i\mathbf{r}\cdot\Delta_i\mathbf{v} - 2|\Delta_i\mathbf{v}|^2) - \Delta_i\mathbf{r}\cdot\Delta_i\mathbf{f} + \gamma\Delta_i\mathbf{r}\cdot\Delta_i\mathbf{v}. \tag{13}$$

The left hand side contain the tensions, which are unknowns, but the rest of the variables and the right hand side are all known. These equations form a tridiagonal matrix equation which can be solved for the $t_i$'s in a time $O(N)$.

After the tensions are determined, they are used in the right hand side of Eq. (7). These $2N$ first order differential equation can be integrated by a variety of methods. This paper uses fourth order Runge Kutta to do this. Excluding the operations involving the computation of the forces $\mathbf{f}$, this algorithm runs in $O(N)$ operations per time step. For short range potentials, such as are used here, the forces also require $O(N)$ operations, meaning the operations per time step are $O(N)$. This scales the same way with $N$ as nonconstrained simulations such as molecular dynamics with variable bond lengths.

In general, this algorithm can be easily extended to systems with any set of connections between masses, such as branched topology. For the simplest variant, the ring chain, we modify the problem by introducing fictitious particles $\mathbf{r}_{N+1}\equiv\mathbf{r}_1$, and $\mathbf{r}_0\equiv\mathbf{r}_N$. This places an additional link between monomer 1 and $N$, giving rise to an additional tension $t_N$. To keep the form of the equations the same, it is convenient to introduce $t_0\equiv t_N$. In this case Eq. (13) becomes a cyclic tridiagonal system of equations that can be easily solved as well. However for more general connections, the order of the number of operations will be greater than $N$.

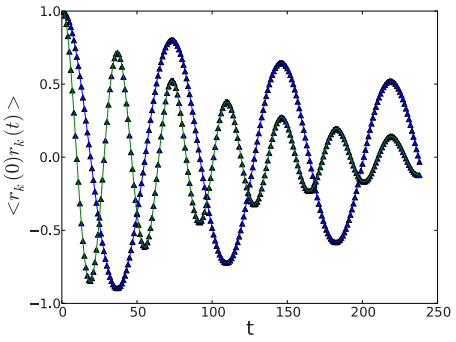


FIG. 1. (Color online) Correlation functions for a freely hinged chain in a vacuum for $N=64$ for the lowest two modes, shown by the solid triangles. The line going through them are fits using Eq. (6).

Typically, the step size used in this work for a Runge Kutta iteration was 0.01. Therefore this algorithm provides an efficient method for investigating dynamics of a polymer in a vacuum.

## III. SIMULATIONS

We first consider the case where there are no potentials but only the freely hinged constraint. In this work, we consider a step length $l=1$ and at temperature $k_BT=1$. We fit the correlation functions for numerical data for $N=64$ using Eq. (6). The first two mode are shown in Fig. 1 As can be seen, the fit to the data is excellent. This was averaged over 37 578 runs, so that the error bars on the data are negligible. Clearly for this range of parameters, the decay of a single $k$-mode is well described by a damped harmonic oscillator. All data for correlation functions shown are normalized to unity at $t=0$. This is because the amplitude of the modes is proportional to $1/k^2$, making it hard to discern the data without this rescaling.

It is important to note that in general, this kind of correlation function cannot be described by a single mode, and that the answer is expected to be the sum over a large number of modes. In fact, for strong enough dihedral potentials more modes need to be included, however we shall see that for quite strong potentials, a single mode fits the simulation data quite well.

The parameters for the oscillator can be fit as a function of $k$. $\Omega_k$ is first determined and then the corresponding parameters in Eq. (5), $M/K$ and $\nu/K$ are calculated. In Fig. 2, $M$ and $\nu$ were fitted for different mode numbers $k=\pi n/N$ with $N=256$ (the step length has been set to unity). The fluctuations give a measure of the uncertainty in this data as was checked by fitting with independent data.

Note that according to Eq. (2), both curves should be constant as a function of the mode number. However a clear variation is seen in each. The effective mass of the mode increases with increasing $k$, and the effective friction coefficient is not $\propto k^2$, but is slightly less. The data could be fit

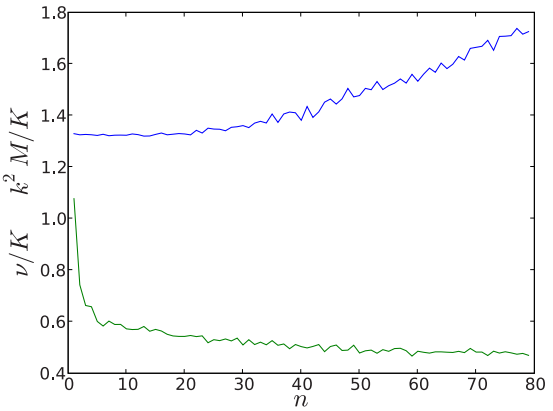


FIG. 2. (Color online) The parameters for fits of the time autocorrelation function, Eq. (6). to a damped harmonic oscillator are shown for a freely hinged chain with $N=256$. The upper line represents the mass $k^2M/K$ of each mode, and the lower curve represents that damping $\nu/K$.

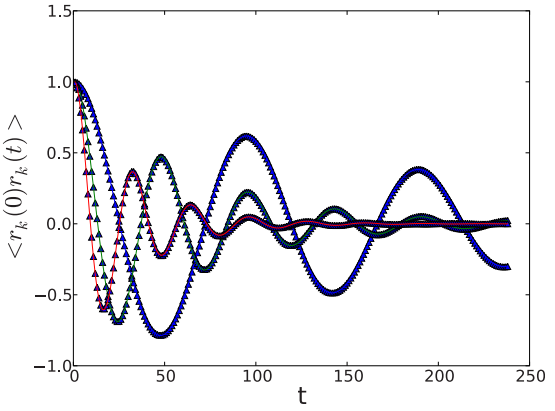


FIG. 3. (Color online) Time autocorrelation functions where bond angle is now restricted for $N=64$. Data for the first three modes is shown by the solid triangles. The lines going through it is a fit using Eq. (6).

equally well, with a slightly smaller exponent so that $\nu \propto k^p$ with $p<2$, or as a logarithmic correction, $k^2/\log(k)$. In either case, the assumption of a local term for the friction is apparently not completely correct. There is a subtle transfer of energy between modes leading to nonlocality. The same is apparently true for the mass, and no doubt these two effects are related. The goal of the present work is not to explain these effects theoretically, but to investigate how the friction coefficient is altered by local potentials along the chain. Therefore we will now turn our attention to this problem.

The oscillations seen are a result of the weak form of damping at low wave number. Do these persist if the chain is no longer freely hinged? To answer this, we first examine a model where the distribution of bond, or valency angles, is weighted around a set of values centered at a particular angle $\theta_V$. To restrict configurations in this manner, a potential is constructed between the nearest neighbors of monomer $i$ as follows:

$$U_{val} = \frac{U_b}{4}(|\mathbf{r}_{i+1} - \mathbf{r}_{i-1}|^2 - r_0^2)^2. \tag{14}$$

Because the distance between nearest neighbors is fixed, for large $U_b$, this will limit configurations as just described. $r_0$ is chosen to give the value of $\theta_V$ desired, in this case $\theta_V = 104°$. This value is somewhat arbitrary and varies according to the chemical structure of the polymer. As a result, the dynamics will be restricted as well. Figure 3 shows the time autocorrelation function for $U_b=10$, for the first three modes. In this case we see again that the fit to Eq. (6) is excellent. The long wavelength modes are still quite underdamped. A fit of the harmonic oscillator parameters is shown in Fig. 4. It is similar to the freely hinged case, Fig. 1, suggesting that the variation of the drag coefficient with $k$ may be understandable by some general mechanism.

Usually as a link is rotated, there are three energy minima as a function of the dihedral angle. To make this model more realistic, it is necessary to add such a dihedral potential. As a function of the dihedral angle $\theta$, between two adjacent monomers, the potential energy $U=V_d\cos(3\theta)$. This can be expressed in terms of $\cos\theta$ using the usual trigonometric identity. If the bond angle is fixed, $\cos\theta$ can be expressed in terms of dot products which is computationally advantageous. Because the bond angle is almost constant, we still use the same dot product formula in the simulation. This also breaks symmetry between the three minima moving the trans state slightly relative to the two gauche states. This is also seen in real data such as for polyethylene [23]. Figure 5 shows the distribution of bond angles, $\rho(\theta)$, for two separate dihedral potentials, with $V_d=3$ and $V_d=4$, for $U_b=10$ and $N=64$. As the amplitude of the dihedral potential, $V_d$ increases, the ratio of the maximum for the distribution, $\rho_{\max}$ to the minimum $\rho_{\min}$ increases. In these simulations the energy scale was chosen so that the temperature is 1 and Fig. 6 shows that $\log(\rho_{\max}/\rho_{\min}) \approx 2V_d$, It is reduced from approximately $4V_d$ because of coupling to other degrees of freedom such as bond angle. For a real temperature of 330 K, comparison with earlier modeling [24] of polyethylene, yields that $V_d \approx 2.5$ (as we are using units where $T=1$.) At lower

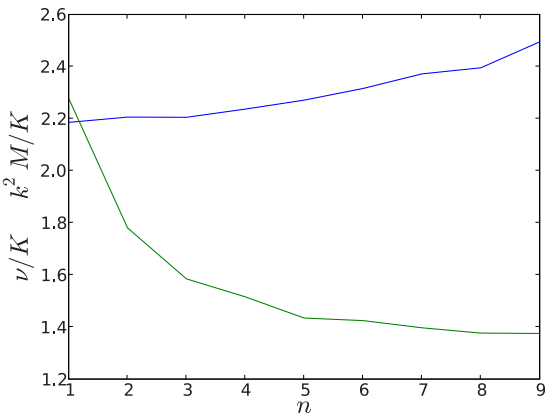


FIG. 4. (Color online) The parameters for fits of the time autocorrelation function, Eq. (6), to a damped harmonic oscillator are shown for the same data as in Fig. 3. The upper curve is a measure of the mass $k^2M/K$, and the lower curve is measure of the damping $\nu/K$.

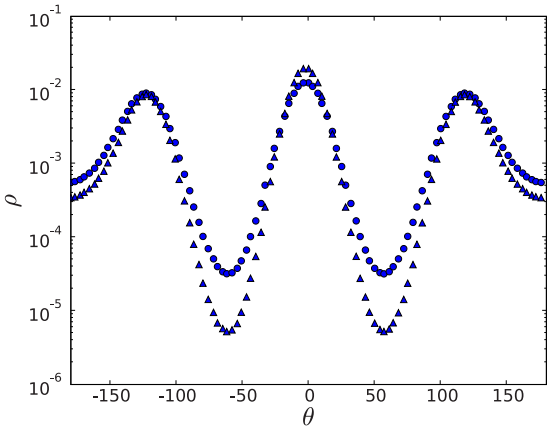


FIG. 5. (Color online) The distribution of dihedral bond angles for two different heights of the dihedral potential, $V_d$=3 (circles) and $V_d$=4 (triangles). Here $U_b$=10 and $N$=64.

real temperatures, the potential will be correspondingly higher.

Figure 7 shows the correlation function fit to the damped harmonic oscillator for $V_d$=2 (a), and $V_d$=3 (b). Here $N$=64 and $U_b$=10. In both cases, clear oscillations can be seen for the lowest modes.

It is of interest to know how the frequency dependent damping depends on the height of the dihedral potential. Figure 8 shows the results of fitting different modes to the damped harmonic oscillator, taking into account the possibility of both underdamped and overdamped motion. As with Fig. 2, the damping $\nu$ is divided by $K \propto k^2$. The nonconstant nature of the results show that for quite substantial $V_d$, there is a similar deviation from the expected Kelvin damping as was seen in Figs. 2 and 4. Note that even if higher modes are overdamped we expect the for lower enough $k$, and long enough chains, the motion will become underdamped. This is because of the $k$-dependent form of the damping $\nu$, which goes to zero for as $k \to 0$.

As can be seen from Fig. 6, for $V_d > 1$, barriers to rotation are substantial. It would then first appear that motion would be much more like that of a lattice model, where a monomer stays in a potential minimum for a long time and flips to

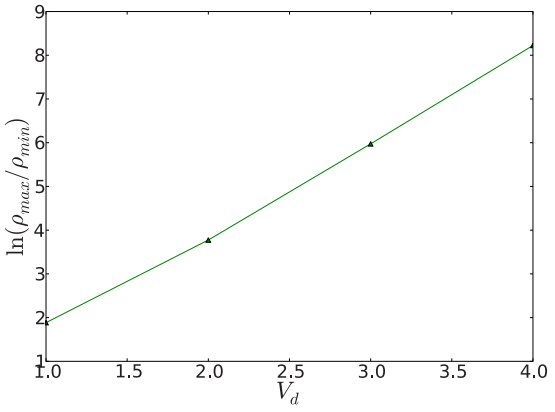


FIG. 6. (Color online) The natural logarithm of the dihedral angle distribution maximum to minimum as a function of potential amplitude $V_d$ with $U_b$=10.

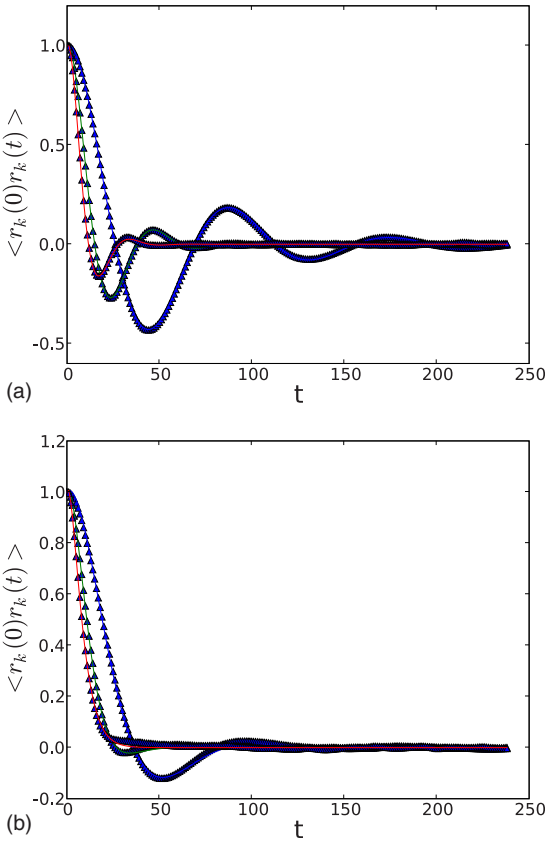


FIG. 7. (Color online) Time autocorrelation functions where bond angle and a dihedral potential for $N$=64, $U_b$=10. Data for the first three modes are shown by the solid triangles. The lines going through it is a fit using Eq. (6). (a) with $V_d$=2 and (b) with $V_d$=3.

another state. This would suggest that the motion would be heavily overdamped, with correlation functions like those of the Rouse model. However we have seen that even in these cases, the motion for long wavelengths, is underdamped. For strong enough potentials such as $V_d$=4, the motion even at long wavelengths and $N$=64, ceases to be underdamped. The relaxation becomes very slow and does not fit well to a

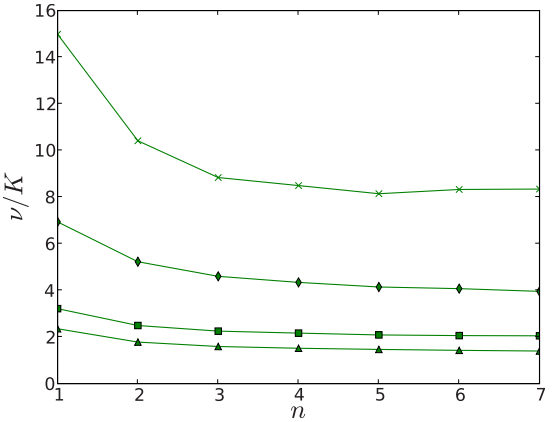


FIG. 8. (Color online) The damping as a function of mode number for a range of dihedral potentials with $N$=64. The bottom curve shown by the triangles is $V_d$=0, the next highest, $V_d$=1 (squares), then $V_d$=2 (diamonds), and $V_d$=3 (crosses).

simple harmonic oscillator. Many more frequency modes must be considered in this case. However as we argued above, for long enough chain length, we expect to see underdamped motion for low $k$. When the value of $U_b$ is increased, this increases $\log(\rho_{\max}/\rho_{\min})$ and will make the barrier height larger. Still for $N=64$, when the dihedral constant $U_b$ is raised to $U_b=40$, oscillations persist when $V_d=2$.

## IV. CONCLUSIONS

These results are of interest for two reasons. First, it sheds like on the nature of internal friction of polymer chains in solution. This work characterizes the nature of this dissipation. It is quite similar to that of Kelvin friction, Eq. (1). However it is not identical as the damping is larger for small wavenumber. This departure is at present unexplained and is probably quite nontrivial to understand as it is related to the dynamics of nonlinear one dimensional chains [11,12].

Second, it is important in the understanding the internal dynamics of polymers in a vacuum of which there is at present little experimental or theoretical understanding. In reality polymers in this situation will be charged and have van der Waals interactions. An investigation of these have shown that their effects are very important [7]. However as with the understanding of ideal chains in polymer solutions, it is important to understand an ideal chain in a vacuum as the starting point for further analysis.

## ACKNOWLEDGMENT

The author thanks Onuttom Narayan for useful discussions.

[1] P. G. de Gennes, *Scaling Concepts in Polymer Physics* (Cornell University Press, Ithaca, New York, 1985).
[2] R. Cerf, C. R. Acad. Sci. Paris **286B**, 265 (1978).
[3] R. Cerf, C. R. Acad. Sci. Paris **230**, 81 (1950); J. Leray, Ph.D. thesis, University of Strasbourg, 1959.
[4] D. A. MacInnes, J. Polym. Sci. **15**, 465 (1977); **15**, 657 (1977).
[5] P. G. de Gennes, J. Chem. Phys. **66**, 5825 (1977).
[6] F. Hillenkamp, *MALDI MS: A Practical Guide to Instrumentation, Methods and Applications*, edited by J. Peter-Katalinic (Wiley, New York, 2007).
[7] J. M. Deutsch, Phys. Rev. Lett. **99**, 238301 (2007).
[8] J. M. Deutsch, Phys. Rev. E **77**, 051804 (2008).
[9] M. P. Taylor, K. Isik, and J. Luettmer-Strathmann, Phys. Rev. E **78**, 051805 (2008).
[10] A. Mossa, M. Pettini, and C. Clementi, Phys. Rev. E **74**, 041805 (2006).
[11] E. Fermi, J. Pasta, and S. Ulam, *Studies of Nonlinear Problems* (Los Alamos Document LA-1940, 1955).
[12] For a review see G. P. Berman and F. M. Izrailev, Chaos **15**, 015104 (2005) ; and references therein.
[13] O. Narayan and S. Ramaswamy, Phys. Rev. Lett. **89**, 200601 (2002).
[14] J. M. Deutsch and O. Narayan, Phys. Rev. E **68**, 010201 (2003); **68**, 041203 (2003).
[15] B. J. Alder and T. E. Wainwright, Phys. Rev. A **1**, 18 (1970).
[16] K. Carneiro, Phys. Rev. A **14**, 517 (1976).
[17] Ya. G. Sinai and N. I. Chernov, Russ. Math. Surveys **42**, 181 (1987).
[18] T. Mai, A. Dhar, and O. Narayan, Phys. Rev. Lett. **98**, 184301 (2007).
[19] J. P. Sethna, *Statistical Mechanics Entropy, Order Parameters and Complexity* (Oxford University Press, New York, 2006), p. 210.
[20] P. E. Rouse, J. Chem. Phys. **21**, 1272 (1953).
[21] J. M. Deutsch, Science **240**, 922 (1988).
[22] J. M. Deutsch and T. M. Madden, J. Chem. Phys. **90**, 2476 (1989).
[23] D. Campbell, R. A. Pethrick, and J. R. White, *Polymer Characterization: Physical Techniques*, 2nd ed. (CRC, Boca Raton, 2000), p. 91.
[24] R. H. Boyd, R. H. Gee, J. Han, and Y. Jin, J. Chem. Phys. **101**, 788 (1994).